ResearchGate

See discussions, stats, and author profiles for this publication at: https://www.researchgate.net/publication/231390941

Importance of Biomass Particle Size in Structural Evolution and Reactivity of Char in Steam Gasification

ARTICLE *in* INDUSTRIAL & ENGINEERING CHEMISTRY RESEARCH · NOVEMBER 2009

Impact Factor: 2.59 · DOI: 10.1021/ie901214z

CITATIONS
10

READS
30

5 AUTHORS, INCLUDING:

Mohammad Asadullah
Universiti Teknologi MARA
84 PUBLICATIONS **2,100** CITATIONS
SEE PROFILE

Shu Zhang
23 PUBLICATIONS **415** CITATIONS
SEE PROFILE

Zhenhua Min
Curtin University
13 PUBLICATIONS **238** CITATIONS
SEE PROFILE

Available from: Mohammad Asadullah
Retrieved on: 30 January 2016

Importance of Biomass Particle Size in Structural Evolution and Reactivity of Char in Steam Gasification

Mohammad Asadullah,[†,‡] Shu Zhang,[†,‡] Zhenhua Min,[†,‡] Piyachat Yimsiri,[†] and Chun-Zhu Li*[,†,‡]

Department of Chemical Engineering, Monash University, VIC 3800, Australia, and Curtin Centre for Advanced Energy Science and Engineering, Curtin University of Technology, 1 Turner Avenue, Technology Park, WA 6102, Australia

An Australian mallee wood of different particle sizes was gasified in steam in a fluidized-bed reactor at different temperatures. The structural features of chars, combustion reactivity of chars, and alkali and alkaline earth metallic (AAEM) species retention in chars were investigated in view to elucidate how the particle size affects the carbon conversion during steam gasification of biomass. The structural features and combustion reactivity of chars were investigated using Raman spectroscopy and thermogravimetric anlysis, respectively. The Raman intensity and combustion reactivity of chars were seen to decrease with increasing temperature. However, the combustion reactivity of char increased with increasing biomass particle size in the bigger particle range (1.5−5.18 mm). This is due mainly to the increase of catalytic species (AAEM) retention in chars. The increased AAEM retention and condensation of aromatic ring systems are a result of increasing mass transfer resistance in bigger particles of biomass.

Introduction

Steam gasification of biomass is one of the emerging technologies to meet growing demands of electricity generation, fuels for hydrogen fuel cell, chemicals, and liquid fuels.[1] The process has a number of advantages with respect to sustainable development. However, steam gasification of biomass faces a number of technical challenges to become a commercial renewable energy technology. Char conversion to gas is one of the most important challenges. In the steam gasification system, when biomass is exposed to high temperatures (>700 °C), a complex mixture of steam, vapors of a number of organic compounds, and gaseous products evolves, leaving behind a carbon skeletal solid mass (char). The organic vapors and char then take part in the gasification reaction at sufficiently high temperature in the presence of gasifying agents. In the devolatilization step, about 10−20 wt % char is formed depending on the temperature and biomass particle size. Thus, the overall efficiency of the gasifier directly depends on the conversion level of char in the gasification step.[2]

In the steam gasification of biomass, the primary reaction is between carbon in char and oxygen in steam to form carbon monoxide. Thus the reactivity of carbon in char is important in reaching rapid conversion of char to gas. It is influenced by the char structure at the molecular level[3,4] as well as the deposition of catalytic species such as alkali and alkaline earth metallic species (AAEM) in the carbon skeleton of char.[5−7] During the thermal decomposition of biomass, the organic molecules of biomass rearrange to form the microcrystalline structure of char.[8] Simultaneously, the organic and AAEM vapors are readsorbed on the inner and outer surfaces of the porous char during intraparticle mass transfer. Interparticle readsorption of volatiles also takes place. The deposited species have a great influence on the char structure as well as the reactivity in the gasification step. Thus the reactivity of char[9] is jointly affected by the structure of carbonaceous matter,[3,4] the concentrations of alkali and alkaline earth metallic (AAEM) species acting as inherent catalysts,[5−7] and the physicochemical forms and dispersion of AAEM species in the char.[10] The char structure actually, in turn, determines how the species physicochemically locate inside the carbon skeleton. In addition, the contact of steam with char in the steam gasification step drastically changes the char structure and reactivity.[11] Therefore, it is essential to realize the importance of the structural features of char prepared in steam gasification of biomass under different conditions for the development of biomass conversion technologies for energy.

Biomass has a highly heterogeneous structure with high oxygen content. The fast pyrolysis of biomass, especially at low temperature (e.g., <900 °C), would produce an extremely reactive char, which could be gasified rapidly upon contacting with reactive gasifying agents (e.g., H_2O). However, in fact, the biomass char structure drastically changes and reactivity suddenly falls due to a change of external conditions, e.g., attacking by gasifying agents during steam gasification.[11] During the progress of steam gasification, there is a competition between gas-forming reactions and condensation reaction from small ring systems to larger ring systems. The larger ring systems become increasingly refractive in nature. Understanding the changes in char structure has been made difficult by the lack of suitable analytical techniques to quantify the carbon-skeleton structural features of biomass char.[12]

The structural features of coal chars have been investigated using X-ray diffraction (XRD), Fourier transform infrared (FT-IR) spectroscopy, high-resolution transmission electron microscopy (HRTEM), and Raman spectroscopy.[13−17] The XRD technique is suitable to characterize graphite-like carbon material, having a highly ordered crystalline structure. However, it is evident that the biomass chars are highly disordered carbonaceous materials that may have a short-range-ordered polycrystalline structure with structural defects.[18] The FT-IR spectroscopy precisely identifies the oxygen-containing functional groups in carbon material; however, it is of limited use in exploring the less-polar aromatic structures. Raman spectroscopy is widely used for the characterization of both crystalline and amorphous carbons, because it is sensitive to both of them.[13−17] A novel Raman spectroscopic method has

* To whom correspondence should be addressed. Tel.: +61 8 9266 1131. Fax: +61 8 9266 1138. E-mail: Chun-Zhu.Li@curtin.edu.au.
† Monash University.
‡ Curtin University of Technology.

10.1021/ie901214z CCC: $40.75 © 2009 American Chemical Society
Published on Web 08/27/2009

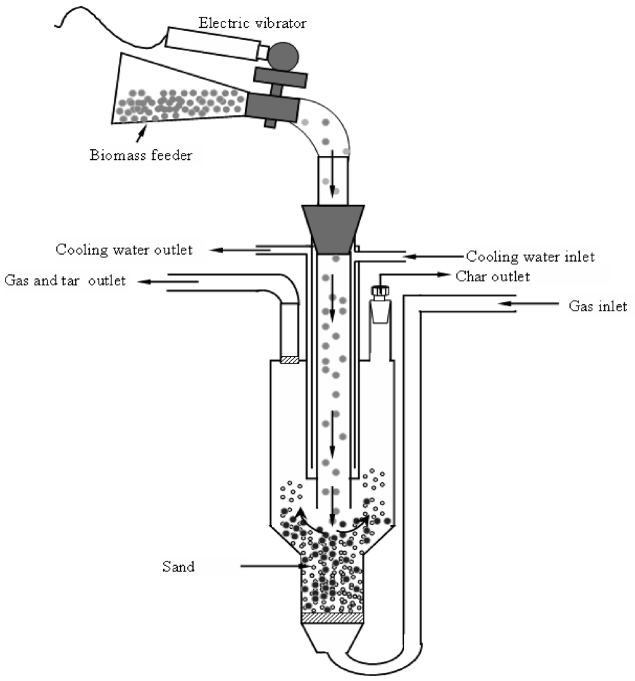

Figure 1. Schematic diagram of the fluidized-bed reactor used for the fast heating pyrolysis.

been developed in our group to characterize the amorphous carbon that will be used in this study to provide information about char structures.[19,20]

To elucidate the changes in char structure and reactivity when a char from the pyrolysis of mallee wood biomass is contacted with steam, different types of chars under different conditions are prepared and investigated with Raman spectroscopy and thermogravimetric analysis (TGA). Our results exhibited that the particle size of biomass has a great role in char structure and reactivity in steam gasification.

Experimental Section

Experimental Procedure for Char Preparation in Steam Gasification. Different particle sizes of mallee wood of Western Australia have been used. Details of the feedstock can be found elsewhere.[21] Steam gasification of biomass has been carried out in a novel quartz reactor, shown in Figure 1. The reactor mainly consists of two parts: the top part is the feeding section and the bottom part is the reaction section. A quartz tube of 14 mm internal diameter is inserted into the reactor through which biomass is fed into the fluidized sand bed. Under the stationary condition, the opening of the feeding tube was just 2 mm above the sand bed. However, during operation it was completely embedded in fluidized sands due to bed expansion on fluidization. Biomass particles fed through the inner tube were carried with argon gas and penetrated inside the sand bed. Before feeding, the reactor was heated to a target temperature. Then the steam was introduced through the bottom of the reactor at a rate of 15 vol % argon flow. The argon gas flow was reduced and adjusted to maintain the same fluidization rate of sand particles. When all the parameters were stabilized, the feeding of biomass into the reactor from the feeder was started with the help of an electric vibrator. About 4.5−5.0 g of biomass was fed within 30 min. Then the feeding of biomass and flow of steam were stopped and the reactor was immediately lifted out of the furnace and cooled naturally with flowing argon. The chars were collected from the reactor through the char outlet tube. The total char was divided into two parts; one was ground to make a homogeneous mixture of chars of different residence time, which was used for characterization.

Char Characterization. A Perkin-Elmer Spectrum GX FT-IR/Raman spectrometer equipped with an excitation laser of 1064 nm was used for structural evaluation of chars using a method developed in our group.[22,23] For Raman analysis, the char sample was diluted and ground with IR grade KBr to a concentration of 0.5 wt % from which the highest total intensity was achieved. An InGaAs detector operated in liquid nitrogen was used to collect Raman scattering using a backscattering configuration. To get detailed information about specific structure from the Raman spectra, the broad band was deconvoluted into 10 Gaussian bands[22] and the assignment of each band may be found elsewhere.[23] The large aromatic ring systems (not less than six fused rings) in chars are represented by the D band, while G_r, V_l, and V_r bands mainly represent the three to five fused rings, methylene or methyl semicircle breathing of aromatic rings, and methyl semicircle breathing of aromatic rings in chars, respectively. The most significant information is obtained from the intensity ratio $I_D/I_{(G_r+V_l+V_r)}$, which expresses the ratio between big and small aromatic ring systems in chars.

For the determination of AAEM retention, 40 mg of char was directly digested in a 1:2:6 mixture of HF, H_2O_2, and HNO_3. A Microwave Digestion System (Multiwave 3000, Anton Paar) was used to carry out the sample digestion at around 200 °C for 45 min. The autogenous pressure of the vessel was about 60 bar. Clear solutions were obtained after digestion. The solvent mixture was then evaporated at 60 °C to complete the dryness of residue. Following the evaporation, the residue was redissolved in 0.02 M methylsulfonic acid (MSA) solution. An ion chromatograph (Dionex) equipped with a CD25 conductivity detector was used to quantify the AAEM species.

Specific reactivity of char was measured using a Perkin-Elmer Pyris 1 thermogravimetric analyzer in air at 370 °C using our previous method.[22] In this investigation, an empty platinum crucible was placed on the holder and heated to 110 °C under N_2 flow with holding for 30 min before the balance reading was tared to zero. About 4 mg of char sample was then loaded into the crucible at room temperature and heated again to 110 °C. The sample was kept at 110 °C under N_2 flow with holding for another 30 min to remove moisture completely from the char, and the balance reading was considered as the mass of dry char. The temperature of the furnace was then increased to 370 °C at a heating rate of 50 °C/min. After stabilization of temperature, the atmosphere for the sample was switched quickly to air from N_2. This analyzing temperature was optimized by trial and error method. Enough time was allowed for maximum char conversion at 370 °C, and then the temperature was increased to 600 °C to burn off the residual carbon completely (holding time 30 min). Finally, the residual mass was considered as the mass of ash. The specific reactivity (R) of char was calculated using the following equation:

$$R = -\frac{1}{W}\frac{dW}{dt}$$

where W is the mass (daf basis) of the char at any given time.

Results and Discussion

Effects of Biomass Particle Size on Char Yield in Steam Gasification. The steam gasification of biomass of different particle sizes has been carried out at different temperatures ranging from 700 to 900 °C. Figure 2 shows the char yields as

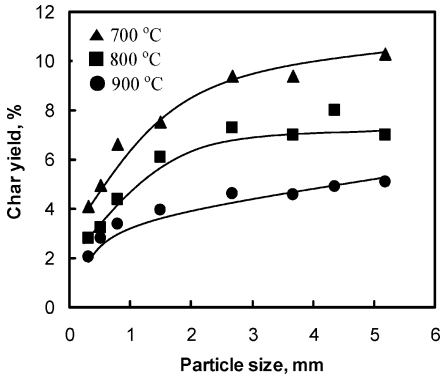

Figure 2. Effects of biomass particle size on char yields at different temperatures in steam gasification.

a function of biomass particle size as well as temperature in steam gasification. As Figure 2 shows, both the particle size and temperature have significant effects on char yields. Higher temperature is favorable for both the devolatilization and steam gasification of char, and thus the char yield at higher temperature is lower. However, the increasing yield of char with increasing particle size is one of the important matters to be discussed. Different types of physicochemical phenomena during devolatilization and steam gasification of char may have been affected due to increase in particle size, affecting the char yields. First, the intraparticle mass transfer resistance increased with increasing biomass particle size. The devolatilization at 700 °C and above is considered as fast pyrolysis where the concentration of volatiles in the char matrix suddenly increases and it is more severe in the bigger particle size. The large tar concentration implies extensive recombination of tarry compounds on the internal surface of the char, resulting in reduced weight loss of char. Second, the increasing distance from outer surfaces to the center of the particles increases the difference of temperature distribution. The most remote part of the particle from the outer surface where the hot sand was first contacted always experienced lower temperature.

The temperature gradient is generated in fact by two reasons. First, the transportable heat is consumed by the endothermic initial pyrolysis process, and second, the lower thermal conductivity of wood particles slows down the heat transfer from the outer into the inner parts of the particles. Therefore, the heating rate of the central mass is much slower than that of the outer mass. This implies that the devolatilization of central mass is slower, leading to the recombination of volatiles. On the other hand, the time required for complete gasification of solid char in steam within the range of experimental temperatures is much higher (some times more than 1 h) than that of the pyrolysis time (<1 s). Literature shows that the external mass transfer of the gases is much faster than the steam gasification.[24] This implies that the gases have enough time to penetrate into the whole particle before the reaction takes place, and thus it is assumed that the steam gasification occurs uniformly over the whole residue. This also suggests that the gasification is kinetically controlled and thus the temperature is the main factor for the increasing carbon conversion with increasing temperature. The particle size range used in this experiment has no effect on the carbon conversion as described elsewhere.[24]

Reactivity of Char Measured in Air at 370 °C. The specific reactivities of chars prepared from different particle sizes of biomass after steam gasification at different temperatures ranging from 700 to 900 °C were determined using a TGA in air at 370 °C. The specific reactivity profiles are depicted in Figure 3 as a function of char conversion. The data in Figure 3 represent

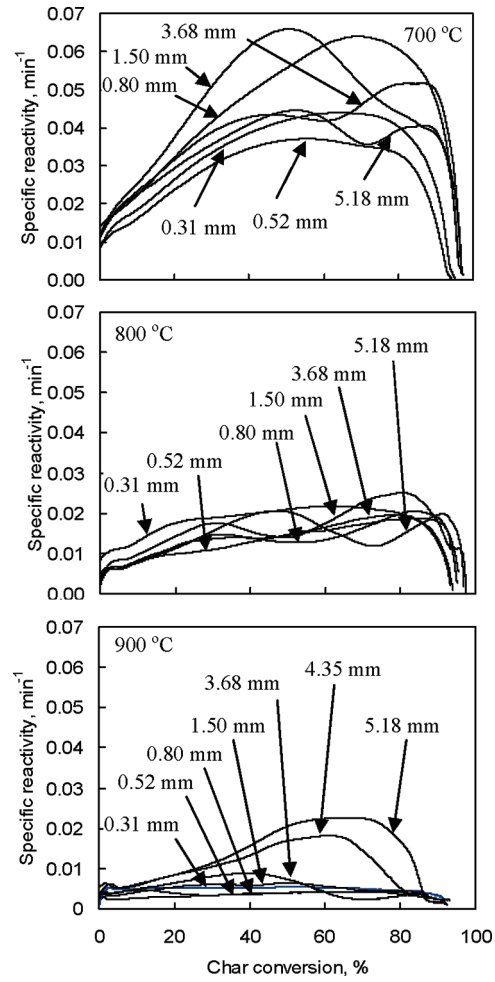

Figure 3. Char reactivity as a function of char conversion measured at 370 °C. The chars were prepared from different biomass particle sizes at different temperatures in steam gasification.

that the reactivities of char prepared at 800 and 900 °C are very close; however, they are much lower than that of the char prepared at 700 °C. This implies that the char prepared at 700 °C is very reactive and the contact of steam with char derived in the pyrolysis zone in the gasifier could not significantly change the reactive physicochemical form of carbon species. In fact, steam gasification of solid carbon species usually takes place above 700 °C.

The reactivity of char prepared from the 0.52 mm average particle size at all temperatures showed the lowest reactivity. The char derived from the smallest particle (0.31 mm) exhibited slightly higher reactivity than 0.52 mm. The reactivity increased with increasing particle size in the bigger particle range. The most notable feature of the data in Figure 3 is that the reactivity curve for smaller chars are almost flat; however, the reactivity curves for chars from particles bigger than 0.52 mm prepared at 800 and 900 °C are peculiarly wave shaped. This is also seen for 700 °C chars prepared from biomass particles bigger than 1.5 mm. This could imply that the reactivity factors, i.e., catalyst (AAEM) concentration and structural features, are almost homogeneous throughout the char from smaller particles. For the chars from bigger particles, the fluctuated reactivity of the same char at different conversion levels reveals that the different domains with distinct structural features in char are formed in which catalyst species are distributed heterogeneously. The heating rates at different places in bigger particles of biomass are different, which could lead to the formation of different

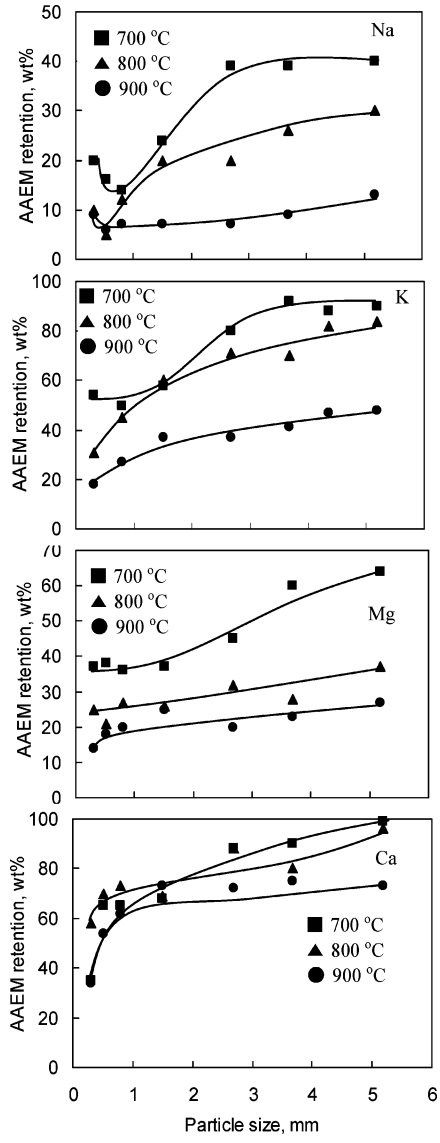

Figure 4. AAEM retentions in chars as a function of biomass particle size. The chars were prepared at 700, 800, and 900 °C in steam gasification.

carbonaceous domains with different reactivities. The more condensed structure and deformed amorphous structure may form two distinct domains. The condensed structure is reasonably less reactive than the amorphous structure. In addition, the existence of catalytic species in condensed carbon species is less preferable and thus they might be enriched in the amorphous domain, leading to higher combustion reactivity in TGA. Furthermore, when amorphous carbon was exhausted in the combustion reaction, the catalyst species moved to the surface of the condensed domain, resulted in higher reactivity of the rest of the carbon, and showed the waving nature of the curve.

Figure 4 represents the AAEM catalyst species (Na, K, Mg, and Ca) retention in chars as a function of biomass particle size. The AAEM retention was calculated based on their contents in dry biomass. Two notable features in the data of Figure 4 have been observed: the AAEM retention in char increased with increasing biomass particle size for all 700, 800, and 900 °C experiments and it decreased with increasing gasification temperature. However, in the case of the smallest (0.31 mm) particle size, the Na retention is slightly higher than that of the next bigger particle (0.52 mm) and the same trend is observed for all three temperatures. For K and Mg, their retentions are almost constant in 0.31, 0.52, and 0.80 mm particles, especially at 700 °C. The effect of higher concentration of catalyst, especially Na in the smallest char particle, could result in higher reactivity, and it was more obvious for 700 °C char as observed in Figure 3. Since the retention of AAEM catalyst species increased remarkably due to the increase of biomass particle size at all temperatures (Figure 4), the reactivity of chars significantly increased as shown in Figure 3 with increasing biomass particle size. Furthermore, since the AAEM retention in chars significantly decreased at elevated temperatures (Figure 4), the reactivity of chars prepared at higher temperatures from the same size of biomass particle reduced to a great extent (Figure 3).

The variability of the retention of AAEM species in char derived from variable particle size of biomass in steam gasification can be understood by the following brief description. In biomass, M (Na, K, Mg, and Ca) exists as inorganic and organic forms. During devolatilization, some extent of AAEM species remain in the carbon matrix and some release in vapor phase. The metal species in the vapor phase recombine by participating in different types of secondary reactions with carbons of both vapor and solid phases in the presence of steam. These processes would proceed by intraparticle and interparticle volatile char interactions. For the smaller particle of biomass, the pressure of vapor phase in the carbon matrix is insignificant due to less mass transfer resistance, and thus the possibility of secondary recombination of AAEM species with carbon inside the particles is less remarkable. However, since the particles of the smallest size (0.31 mm) were light enough to blow up in the gas stream, they were stuck under the top frit through which the upcoming vapor continued to pass and interparticle volatile-char interaction took place. Thus, the Na and K retentions in char from the small biomass particles (especially at 700 °C) are higher, which is reflected in the specific reactivity of char. For bigger particles, although they remained in the sand bed, the AAEM retention is much higher obviously due to intraparticle mass transfer resistance.

Figure 3 also shows different reactivities of the same char at different char conversion levels. Reactivity is less pronounced for all chars at 700 °C and chars from smaller particles at 800 and 900 °C. The variable reactivity of the same char implies that the AAEM distribution in char is heterogeneous due to different structural features of char. Basically, biomass char has two distinct regions as described in detail in the next section: amorphous with a less aromatic region and a condensed polycyclic aromatic region. It is perceived that it could be difficult to retain the AAEM species in the condensed aromatic ring systems and thus the AAEM species moved to the less aromatic region during ring condensation in steam gasification. As a result, the possibility of AAEM concentration is higher in the amorphous region than in the condensed region. During reactivity measurement, the dense catalyst region exhibited higher reactivity. When the carbon of the reactive region was exhausted, the reactivity curve showed the lowest reactivity. Due to continuous exhaustion of carbon, the catalyst species gradually moved to the less reactive region and started to react with polycyclic condensed char and the reactivity curve further showed higher reactivity. This phenomenon is more pronounced for chars prepared from the bigger particles of biomass due to pronounced structural and AAEM distribution heterogeneity.

Structural Change in Char during Steam Gasification. The total Raman peak areas of chars prepared in steam gasification of biomass at different temperatures ranging from 700 to 900 °C from different particle sizes ranging from 0.31 to 5.18 mm are shown in Figure 5. The Raman intensity was taken as the

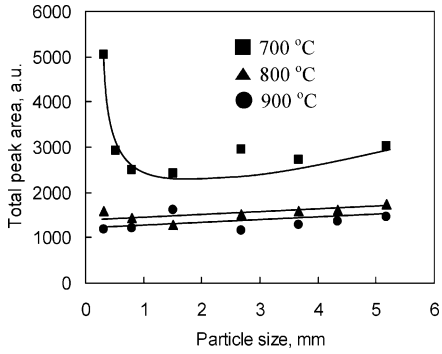

Figure 5. Effects of biomass particle size and temperature on the total Raman peak area of chars prepared in steam gasification.

total peak area in the region 800−1800 cm^{-1}. It can be seen that the differences in total peak areas among the char samples decreased significantly with increasing gasification temperature, regardless of the particle size of the biomass. However, the total Raman intensity for the char prepared at 700 °C from the smallest particle (0.31 mm) is much higher, which sharply decreased with increasing particle size up to 0.8 mm. Further increase of the particle size resulted in a gradual increase of total Raman intensity.

To gain clear insight about the critical structural features, Raman spectra of different chars prepared from 4.38 mm average particle size are curve fitted as shown in Figure 6. It can be noted that the intensity of all Gaussian bands was drastically decreased from 700 to 800 °C; however, it was slightly decreased from 800 to 900 °C. This implies that the release of O-containing functional groups and condensation of ring systems during steam gasification of char is more pronounced at 800 °C. In fact, the gasification of biomass in steam is spontaneous at 800 °C. On the other hand, the G band is always weaker than the G_r, V_r (three to five fused benzene rings), and D (greater than six fused benzene rings) bands, which correspond to the amorphous carbon structures, implying the poor order in chars. Therefore, the ratio between the intensity of the D band and the total intensities of the G_r, V_l, and V_r bands is mainly attributed to the ratio between the large aromatic ring systems (greater than six rings) and the ring systems of three to five aromatic rings.

Figure 7 illustrated the band intensity ratio $I_D/I_{(G_r+V_l+V_r)}$ as a function of biomass particle size at different temperatures. The ratios among these bands provide detailed information about the changes in the structure of biomass char during steam gasification. The group of $G_r + V_l + V_r$ bands mainly represents amorphous carbon structure with especially small aromatics (three to five fused rings). The D band signals condensed and large aromatic ring systems (no less than six fused rings) of chars.[19,20] Furthermore, the band area of V_l and V_r could be also contributed by aliphatics and carboxylates. However, considering the temperature and reaction atmosphere used, it was unlikely for the aliphatics and carboxylates to survive. The ratio $I_D/I_{(G_r+V_l+V_r)}$ remarkably increased with increasing temperature. This can be explained by the fact that the thermal effect at 700 °C could not result in significant ring condensation in char. The ring condensation reaction is spontaneous at 800 °C and above especially in the presence of steam. By the formation of radicals, steam initially opened the ring so that the ring condensation could proceed. The ratio $I_D/I_{(G_r+V_l+V_r)}$ is much higher for all chars prepared at 900 °C, representing that the polycyclic aromatic ring systems are largely formed by expending smaller ring systems.

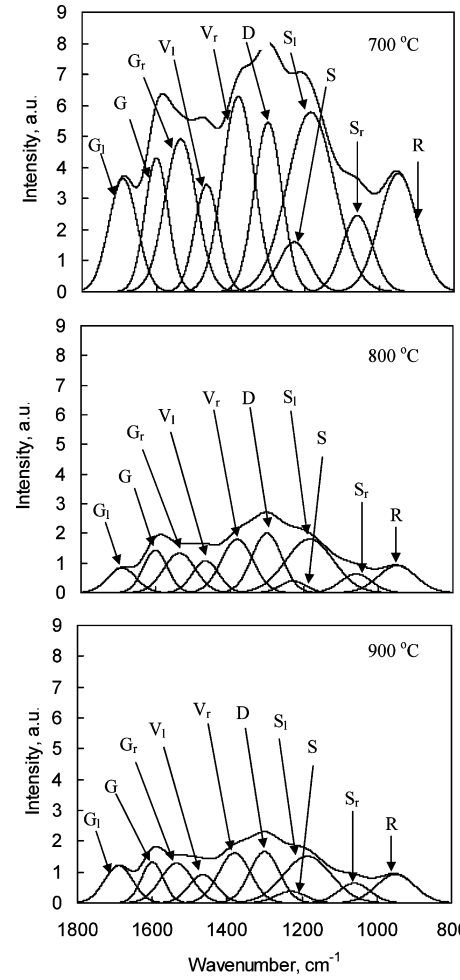

Figure 6. Deconvoluted Raman spectra of chars prepared in steam gasification of biomass of 4.35 mm particle size at different temperatures.

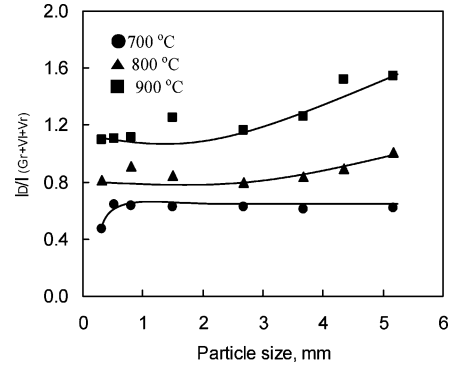

Figure 7. Effects of biomass particle size and temperature on Raman peak area ratio $I_D/I_{(G_r+V_l+V_r)}$.

From Figure 7 it can also be seen that the peak area ratio $I_D/I_{(G_r+V_l+V_r)}$ is almost constant for all chars prepared at 700 °C regardless of particle size; however, it increased gradually with increasing particle size for 800 °C. The increasing trend is more pronounced for 900 °C chars. The increase of particle size increases the resistance against the diffusion of volatiles released from the internal part of the biomass. As a result, the deposition tendency and the recombination of the less aromatic tarry compounds increased, resulting in the condensation of aromatic rings and thus increasing the polyaromatic ring systems. This structure more likely contributed to the D band, so as to increase the $I_D/I_{(G_r+V_l+V_r)}$ ratio with increasing biomass particle size. The

structural heterogeneity between the amorphous structure with less aromatic rings and condensed structures with large aromatic rings becomes more pronounced. Since the condensation of ring systems takes place by releasing small groups and other organic and inorganic particles, it can be realized that AAEM concentration is lower in the condensed part. Alternatively, AAEM accumulated in the amorphous region with smaller ring systems, leading to the higher reactivity in the TGA experiment. When more active carbons exhausted, the catalytic species moved to the comparatively less active carbons, showing further higher reactivity, and generated waving curves especially for chars prepared from bigger particles of biomass at higher temperature as is observed in Figure 3.

Summary and Conclusions

The reactivity of char, generated in steam gasification of biomass, depends on its structural features as well as retention and distribution of catalytic species (AAEM) in char. The reactivity, structures, and retention of AAEM in char were also affected by the biomass particle size and gasification temperature. The variation of temperature can reasonably change the characteristics of char. This is because the severity of reaction conditions can initiate a number of chemical reactions. As a result, the total Raman intensities between 800 and 1800 cm^{-1} were seen to decrease with increasing temperature from 700 to 900 °C for all chars regardless of particle size, due mainly to the increasing aromatization of the chars and loss of O-containing species and substitutional groups. Smaller aromatic ring systems tended to be lost or transformed into large ones with increasing temperature for all chars. In terms of the particle size, the total Raman intensities of char were gradually increased in the bigger particle range. This increment of total peak area is mainly due to the contribution of the D band, which corresponds to a larger aromatic ring system. This implies that the reactivity of char would be reduced. However, it is contrary to the fact that the reactivity mostly increased with increasing biomass particle size. This has been supported by the retention of AAEM species. They increased significantly in char with increasing biomass particle size, which might catalyze the combustion of char significantly.

Acknowledgment

This project received funding from the Australian Government as part of the Asia−Pacific Partnership on Clean Development and Climate.

Literature Cited

(1) Li, C.-Z. Special issue—Gasification: a route to clean energy. *Process. Saf. Environ. Prot.* **2006**, *84*, 407–408.

(2) Hayashi, J.-I.; Hosokai, S.; Sonoyama, N. Gasification of low-rank solid fuels with thermochemical energy recuperation for hydrogen production and power generation. *Process. Saf. Environ. Prot.* **2006**, *84*, 409–419.

(3) Li, X.; Hayashi, J.-I.; Li, C.-Z. Volatilisation and catalytic effects of alkali and alkaline earth metallic species during the pyrolysis and gasification of Victorian brown coal. Part VII. Raman spectroscopic study on the changes in char structure during the catalytic gasification in air. *Fuel* **2006**, *85*, 1509–1517.

(4) Li, X.; Li, C.-Z. Volatilisation and catalytic effects of alkali and alkaline earth metallic species during the pyrolysis and gasification of Victorian brown coal. Part VIII. Catalysis and changes in char structure during gasification in steam. *Fuel* **2006**, *85*, 1518–1525.

(5) Wu, H.; Hayashi, J.-I.; Chiba, T.; Takarada, T.; Li, C.-Z. Volatilisation and catalytic effects of alkali and alkaline earth metallic species during the pyrolysis and gasification of Victorian brown coal. Part V. Combined effects of Na concentration and char structure on char reactivity. *Fuel* **2004**, *83*, 23–30.

(6) Mermoud, F.; Salvador, S.; Van de Steene, L.; Golfier, F. Influence of the pyrolysis heating rate on the steam gasification rate of large wood char particles. *Fuel* **2006**, *85*, 1473–1482.

(7) Zolin, A.; Jensen, A.; Jensen, P. A.; Frandsen, F.; Dam-Johansen, K. The influence of inorganic materials on the thermal deactivation of fuel chars. *Energy Fuels* **2001**, *15*, 1110–1122.

(8) Senneca, O.; Russo, P.; Salatino, P.; Masi, S. The relevance of thermal annealing to the evolution of coal char gasification reactivity. *Carbon* **1997**, *35* (1), 141–151.

(9) Anthony, D. B.; Howard, J. B. Coal devolatilization and Hydrogasification. *AIChE J.* **1976**, *22*, 625–632.

(10) Quyn, D. M.; Wu, H.; Hayashi, J.-I.; Li, C.-Z. Volatilisation and catalytic effects of alkali and alkaline earth metallic species during the pyrolysis and gasification of Victorian brown coal. Part IV. Catalytic effects of NaCl and ion-exchangeable Na in coal on char reactivity. *Fuel* **2003**, *82*, 587–593.

(11) Keown, D. M.; Hayashi, J.-I.; Li, C.-Z. Drastic changes in biomass char structure and reactivity upon contact with steam. *Fuel* **2008**, *87*, 1127–1132.

(12) Li, C.-Z. Some recent advances in the understanding of the pyrolysis and gasification behaviour of Victorian brown coal. *Fuel* **2007**, *86*, 1664–1683.

(13) Green, P. D.; Johnson, C. A.; Thomas, K. M. Applications of laser Raman microprobe spectroscopy to the characterization of coals and cokes. *Fuel* **1983**, *62*, 1013–1023.

(14) Cuesta, A.; Dhamelincourt, P.; Laureyns, J.; Martinez-Alonso, A.; Tascon, J. M. D. Raman microprobe studies on carbon materials. *Carbon* **1994**, *32* (8)), 1523–1532.

(15) Tuinstra, F.; Koenig, J. L. Raman spectrum of graphite. *J. Chem. Phys.* **1970**, *53*, 1126–1130.

(16) van Doorn, J.; Vuurman, M. A.; Tromp, P. J. J.; Stufkens, D. J.; Moulijn, J. A. Correlation between Raman spectroscopic data and the temperature-programmed oxidation reactivity of coals and carbons. *Fuel Process. Technol.* **1990**, *24*, 407–413.

(17) Zerda, T. W.; Xu, W.; Zerda, A.; Zhao, Y.; Von Dreele, R. B. High pressure Raman and neutron scattering study on structure of carbon black particles. *Carbon* **2000**, *38* (3), 355–361.

(18) Sharma, R. K.; Wooten, J. B.; Baliga, V. L.; Hajaligol, M. R. Characterization of chars from biomass-derived materials: pectin chars. *Fuel* **2001**, *80*, 1825–1836.

(19) Li, X.; Hayashi, J.-I.; Li, C.-Z. FT-Raman spectroscopic study of the evolution of char structure during the pyrolysis of a Victorian brown coal. *Fuel* **2006**, *85*, 1700–1707.

(20) Keown, D. M.; Li, X.; Hayashi, J.-I.; Li, C.-Z. Characterization of the structural features of char from the pyrolysis of cane trash using Fourier Transform-Raman spectroscopy. *Energy Fuels* **2007**, *21*, 1816–1821.

(21) Garcia-Perez, M.; Wang, X. S.; Shen, J.; Rhodes, M. J.; Tian, F.; Lee, W.-Z.; Wu, H.; Li, C.-Z. Fast pyrolysis of oil mallee woody biomass: effect of temperature on the yield and quality of pyrolysis products. *Ind. Eng. Chem. Res.* **2008**, *47*, 1846–1854.

(22) Li, C.-Z.; Sathe, C.; Kershaw, J. R.; Pang, Y. Fates and roles of alkali and alkaline earth metals during the pyrolysis of a Victorian brown coal. *Fuel* **2000**, *79*, 427–438.

(23) Luo, C.; Watanabe, T.; Nakamura, M.; Uemiya, S.; Kojima, T. Gasification kinetics of coal chars carbonized under rapid and slow heating conditions at elevated temperatures. *J. Energy Resour. Technol.* **2001**, *123*, 21–27.

(24) Dupont, C.; Boissonnet, G.; Seiler, J.-M.; Gauthier, P.; Schweich, D. Study about the kinetic processes of biomass steam gasification. *Fuel* **2007**, *86*, 32–40.

Received for review July 31, 2009
Accepted August 10, 2009

IE901214Z